Graphene, 2013, 2, 18-34
http://dx.doi.org/10.4236/graphene.2013.21004 Published Online January 2013 (http://www.scirp.org/journal/graphen

Force Field Based MM2 Molecule-Surface Binding Energies for Graphite and Graphene

Jae H. Son, Thomas R. Rybolt*
Department of Chemistry, University of Tennessee at Chattanooga, Chattanooga, USA
Email: *Tom-Rybolt@utc.edu

Received November 11, 2012; revised December 12, 2012; accepted January 11, 2013

ABSTRACT

The gas phase adsorption of 118 organic molecules on graphite and graphene was studied by calculating their molecule-surface binding energies, Ecal*, using molecular mechanics MM2 parameters. Due to the general lack of reported experimental binding energy values for organic molecules with graphene, E*(graphene), it was considered desirable to have a simple but effective method to estimate these values. Calculated binding energy values using a three-layer model, Ecal*(3), were compared and correlated to published experimental values for graphitic surfaces, E*(graphite). Published values of experimental binding energies for graphite, E*(graphite), were available from gas-solid chromatogramphy in the Henry's Law region over a range of temperature. Calculated binding energy values using a one-layer model, Ecal*(1), were compared to the three-layer Ecal*(3) values and found to consistently be 93.5% as large. This relation along with an E*(graphite) and Ecal*(3) correlation was used to develop a means to estimate molecule-graphene binding energies. Using this approach we report estimated values of 118 molecule-graphene binding energy values.

Keywords: Molecule-Graphene Interaction; Molecule-Graphite Interaction; Molecular Mechanics; Adsorption Energy; Binding Energy on Graphene; Binding Energy on Graphite

1. Introduction

Graphene is a now well-known single layer of carbons arranged in a hexagonal configuration. Multiple layers of graphene stacked upon each other and held together by van der Waal forces form graphite. Graphene is of great interest because of its many unique properties [1,2]. Graphene is transparent, light, and an excellent conductor of electricity and heat. Its transparency and electric conductivity are desirable properties for touch screen electronic devices. Graphene's thermal and electrical conductivity outperform copper. At room temperature, copper has a thermal conductivity of 401 $Wm^{-1}\cdot K^{-1}$ while graphene's is 5000 $Wm^{-1}\cdot K^{-1}$ [3]. The electrical conductivity of copper is $0.60 \times 10^6\ \Omega^{-1}\cdot cm^{-1}$ and graphene's is $0.96 \times 10^6\ \Omega^{-1}\cdot cm^{-1}$ [3]. The breaking strength of graphene is approximately 42 N/m and an equivalent thickness, steel has a value of 0.40 N/m [3]. In addition to these striking graphene properties, one promising application of this unique two-dimensional material is as a molecular sensor.

Graphene-based devices have been considered for various electronic and optoelectronic devices as well as gas sensors and biosensors [4]. A single layer of graphene, bilayer of graphene, few-layers of graphene, or modified graphene surface can act as a sensor when a molecule adsorbs on the surface and changes the graphene's electric conductivity or other measureable property. The change in conductivity or other property can then be correlated with amount of molecules adsorbed [5]. For example, the electrical conductivity of a graphene fabricated device was observed to increase linearly with an increase of carbon dioxide in the 10 to 100 ppm range [6].

In order to exploit the potential applications of graphene as gas sensors, the adsorption of a series of small gas molecules on pristine graphene and Si-doped graphene have been investigated by ab initio calculations [7]. Their theoretical results indicated that the electronic properties are sensitive to oxygen and nitrogen dioxide adsorption, but not as much modified by the adsorption of carbon monoxide and water [7]. The adsorption of inorganic molecules including water, ammonia, carbon monoxide, nitrogen dioxide, and nitrogen oxide on a graphene substrate were considered using first-principles calculations [8]. Graphene surfaces and variously modified graphene surfaces have been used to develop gas sensor devices and successfully have been used to detect ammonia [9], sulfur dioxide [10], nitrogen dioxide [11], nitrogen dioxide and ammonia [12], carbon dioxide [6], acetone [13], hydrogen sulfide [14], and hydrogen [15,

*Corresponding author.

16]. A variety of surface modifications have been explored and their detection effects examined [14-20].

Adsorption can be studied theoretically by calculating the adsorption interaction energy (binding energy) of a molecule on the surface. A molecule with higher binding energy should have greater adsorption on the graphene surface. For example, given the same amounts of two different molecules in the gas phase (atmosphere surrounding the graphene sensor surface, for example), the ratio of the amounts of those two molecules physically adsorbed on the surface would be different depending on the relative binding energy. The molecule with the stronger binding energy would be expected to be favored in surface physisorption. Therefore, the study of binding energy is important for developing sensors and correlating sensor responses to amounts physically adsorbed and further correlating these amounts to the actual concentrations in a complex mixed molecule environment around the sensor.

It would be useful to be able to predict single layer graphene binding energies for a variety of organic molecules. There is a lack of gas phase experimental binding energies for organic molecules on graphene. However, there have been many experimental studies relating to molecule adsorption on graphite. Using this molecule-graphite binding energy data, our approach is to study the relationship of calculated and experimental graphite adsorption energies and also of calculated graphite and calculated graphene binding energies. Assuming suitable relations are found then it should be possible to calculate molecule-surface binding energies on graphene or graphite and then predict experimental binding energies of molecules on graphene.

Previous studies showed that MM2 molecular mechanics parameters for atom-carbon van der Waals (vdW) interactions are suitable to effectively predict molecule-carbon surface binding energies [21-25]. In these prior studies of gas-solid interactions, the standard augmented MM2 parameters developed by Allinger [26,27] were used to estimate the binding energies of organic molecules interacting with various model carbon surfaces [21-25]. The adsorption of neutral molecules on a carbon surface is dominated by dispersive van der Waals (vdW) forces. In previous studies [21-25] molecule-surface steric energy differences for an adsorbate molecule adjacent to or far from a model adsorbent surface were used to estimate the energy due to adsorption, the binding energy. Although force field calculations do not reference electronic behavior, they have been widely used for determining minimum energies and optimized molecular geometries [28].

2. Experimental Data

A review of the literature revealed a lack of experimental organic molecule-graphene interaction energies. However, a significant number of organic molecule-graphite interaction energies have been reported. These experiments typically utilized either thermal programmed desorption (TPD) or gas-solid chromatography (GSC). TPD experiments usually give information about multilayer or monolayer desorption and so molecule-molecule interactions cannot be ignored [21]. However, many GSC determinations involved finding the low coverage Henry's constants and so reflect the interaction of isolated molecules with the carbon surface.

Sample gas corrected retention times can be converted to a Henry's law adsorption constant (K_H). In various published studies these Henry law constants were obtained over a range of temperature values [29-42]. A plot of the natural logarithm of K_H versus the reciprocal of the temperature (d ln K_H/d/T) gives a plot whose slope is E*/R where E* is the molecule-surface binding energy or adsorption interaction energy and R is the gas constant. If given as R = 0.001986 kcal·K^{-1}·mol^{-1} then the slope times R gives the E* value in kcal/mol. As E* increases then it indicates stronger molecule surface interactions.

Published Studies using Graphitized Thermal Carbon Black (GTCB) were selected as suitable graphitic adsorbents. A total of 118 different organic molecules with a variety of structures and functionality determined from GSC on suitable graphitic surfaces were identified and are reported in **Table 1**. **Table 1** gives the assigned molecule number, molecule name, chemical formula, reference source for value, experimental value E*, and the organic group to which the molecule is assigned. Experimental binding energy data are reported in various units but were converted to kcal/mol for all comparisons. The experimental binding energies or physisorption interaction energies are commonly reported in eV, meV, kJ/mol, and Kelvin. The conversion factors used were based on the relations 1 kcal/mol = 4.336411 × 10^{-2} eV = 43.36411 meV = 4.184 kJ/mol = 503.217 K.

3. Theory

The energy of a molecule calculated from molecular mechanics, E_{MM}, (augmented MM2 parameters were used in this work) is a sum of covalent and noncovalent energies. The MM2 covalent energy contributions include stretch, stretch-bend, angle, dihedral, improper torsion; and the noncovalent energy contributions include electrostatics, hydrogen-bonding, and van der Waals. The van der Waals interaction energy, E_{vdW}, is a parameter that contributes to the noncovalent bond energy, and the Van der Waals radius of atoms dominates the molecule-graphite and molecule-graphene interactions. If two nonbonded atoms are pushed too close together, they will strongly repel from one other. If they are at a suitable intermediate range, they will experience a mutual attrac-

Table 1. Assigned molecule number, molecule name, chemical formula, reference source for value, experimental value E*, and the organic group to which the molecule is assigned.

Number	Name	Formula	Ref	E*(Graphite) kcal/mol	Group
1	butyl aldehyde	C_4H_8O	29	7.4	aldehyde
2	capron aldehyde	$C_6H_{12}O$	29	10.3	aldehyde
3	capryl aldehyde	$C_8H_{16}O$	29	13.4	aldehyde
4	croton aldehyde	C_4H_6O	29	8.7	aldehyde
5	isobutyl aldehyde	C_4H_8O	29	7.2	aldehyde
6	isovaler aldehyde	$C_5H_{10}O$	29	8.7	aldehyde
7	pelargon aldehyde	$C_9H_{19}O$	29	14.1	aldehyde
8	propyl aldehyde	C_3H_6O	29	6.7	aldehyde
9	valer aldehyde	$C_5H_{10}O$	29	8.8	aldehyde
10	ethane	C_2H_6	30	4.3	alkane
11	n-butane	C_4H_{10}	30	6.8	alkane
12	n-decane	$C_{10}H_{22}$	31	16.1	alkane
13	n-heptane	C_7H_{16}	31	11.7	alkane
14	n-hexane	C_6H_{14}	31	10.3	alkane
15	n-nonane	C_9H_{20}	31	14.6	alkane
16	n-octane	C_8H_{18}	31	13.3	alkane
17	n-propane	C_3H_8	30	5.3	alkane
18	n-1-butene	C_4H_8	30	6.7	alkene
19	n-1-decene	$C_{10}H_{20}$	31	15.3	alkene
20	n-1-heptene	C_7H_{14}	31	11.2	alkene
21	n-1-hexene	C_6H_{12}	31	10.0	alkene
22	n-1-nonene	C_9H_{18}	31	14.2	alkene
23	n-1-octene	C_8H_{16}	31	12.9	alkene
24	allyl alcohol	C_3H_6O	29	6.4	alkyl alcohol
25	heptanol-1	$C_7H_{16}O$	29	12.4	alkyl alcohol
26	hexanol-1	$C_6H_{14}O$	29	10.9	alkyl alcohol
27	Isoamyl alcohol	$C_5H_{12}O$	29	8.5	alkyl alcohol
28	isobutyl alchol	$C_4H_{10}O$	29	7.5	alkyl alcohol
29	isopropyl alcohol	C_3H_6O	29	6.7	alkyl alcohol
30	n-pentanol	$C_5H_{12}O$	29	9.5	alkyl alcohol
31	n-butyl alcohol	$C_4H_{10}O$	29	8.3	alkyl alcohol
32	propyl alcohol	C_3H_6O	29	6.8	alkyl alcohol
33	secondary amyl alcohol	$C_5H_{12}O$	29	8.6	alkyl alcohol
34	secondary butyl alcohol	$C_4H_{10}O$	29	7.6	alkyl alcohol
35	tertiary amy alcohol	$C_5H_{12}O$	29	7.8	alkyl alcohol
36	tertiary butyl alcohol	$C_4H_{10}O$	29	7.2	alkyl alcohol
37	di-n-propylamine	$C_{10}H_{19}N$	32	15.8	alkyl amine
38	dibutylamine	$C_8H_{19}N$	32	13.3	alkyl amine
39	diisobutylamine	$C_8H_{19}N$	32	12.2	alkyl amine

Continued

40	dipropylamine	$C_6H_{15}N$	32	10.3	alkyl amine
41	tri-n-propylamine	$C_{15}H_{33}N$	32	21.3	alkyl amine
42	tributylamine	$C_{12}H_{27}N$	32	17.3	alkyl amine
43	triethylamine	$C_6H_{15}N$	32	8.7	alkyl amine
44	hexyne	C_6H_{10}	29	8.6	alkyne
45	1-aminoadamantane	$C_{10}H_{17}N$	33	10.4	aromatic amine
46	1,3,5-triazine	$C_3H_3N_3$	34	8.0	aromatic amine
47	1,8-dimethyl naphthalene	$C_{12}H_{12}$	35	17.4	aromatic amine
48	2-aminoadamantane	$C_{10}H_{17}N$	33	10.7	aromatic amine
49	2,3-dimethyl indol	$C_{10}H_{11}N$	32	16.9	aromatic amine
50	3-methyl indol	C_9H_9N	32	16.0	aromatic amine
51	alpha-naphthylamine	$C_{10}H_9N$	32	17.4	aromatic amine
52	alpha-phenyl propionitrile	C_9H_9N	32	12.8	aromatic amine
53	alpha-phenylethylamine	$C_8H_{11}N$	32	12.6	aromatic amine
54	aniline	C_6H_7N	32	11.6	aromatic amine
55	Benzonitrile	C_7H_5N	32	11.9	aromatic amine
56	beta-naphthylamine	$C_{10}H_9N$	32	17.6	aromatic amine
57	diphenylamine	$C_{12}H_{11}N$	32	21.1	aromatic amine
58	indol	C_8H_7N	32	15.0	aromatic amine
59	m-toluidine	C_7H_9N	32	13.3	aromatic amine
60	N-methylaniline	C_7H_9N	32	13.6	aromatic amine
61	N,N-diethylaniline	$C_{10}H_{15}N$	32	16.5	aromatic amine
62	N,N-dimethylaniline	$C_8H_{11}N$	32	15.3	aromatic amine
63	O-toluidine	C_7H_9N	32	13.3	aromatic amine
64	p-toluidine	C_7H_9N	32	13.4	aromatic amine
65	Pyrazine	$C_4H_4N_2$	34	8.7	aromatic amine
66	Pyridine	C_5H_5N	34	9.3	aromatic amine
67	1-methyl-naphthalene	$C_{11}H_{10}$	30	15.8	benzene
68	1,2,3,5-tetramethyl	$C_{10}H_{14}$	36	15.8	benzene
69	1,2,4-trimethylbenzene	C_9H_{12}	36	14.5	benzene
70	1,3,5-trimethylbenzene	C_9H_{12}	36	14.3	benzene
71	2,3-dimethylnaphthalene	$C_{12}H_{12}$	35	18.2	benzene
72	alpha-methyl naphthalene	$C_{11}H_{10}$	35	17.0	benzene
73	benzene	C_6H_6	36	8.9	benzene
74	beta-methyl naphthalene	$C_{11}H_{10}$	35	17	benzene
75	biphenyl acetylene	$C_{14}H_{10}$	37	20.6	benzene
76	diphenyl	$C_{12}H_{10}$	36	16.3	benzene
77	ethyl benzene	C_8H_{10}	36	11.2	benzene
78	fluorene	$C_{13}H_{10}$	38	19.4	benzene
79	hexa-methyl benzene	$C_{12}H_{18}$	36	18.7	benzene
80	iso-propyl benzene	C_9H_{12}	36	11.5	benzene

Continued

81	m-xylene	C_8H_{10}	36	12.6	benzene
82	n-pentyl benzene	$C_{11}H_{16}$	36	14.6	benzene
83	n-butyl benzene	$C_{10}H_{14}$	36	13.6	benzene
84	n-propyl benzene	C_9H_{12}	36	12.8	benzene
85	naphthalene	$C_{10}H_8$	36	14.9	benzene
86	o-xylene	C_8H_{10}	36	12.6	benzene
87	p-xylene	C_8H_{10}	36	12.6	benzene
88	para-terphenyl	$C_{18}H_{14}$	39	22.7	benzene
89	penta-methyl benzene	$C_{11}H_{16}$	36	17.4	benzene
90	toluene	C_7H_8	36	10.3	benzene
91	1,3-dichlorobenzene	$C_6H_4Cl_2$	40	12.4	chloro aromatic
92	1,4-dichlorobenzene	$C_6H_4Cl_2$	40	12.7	chloro aromatic
93	2-chlorodiphenyl	$C_{12}H_9Cl$	41	15.8	chloro aromatic
94	2,6-dichlorodiphenyl	$C_{12}H_8Cl_2$	41	16.2	chloro aromatic
95	2,6,2-trichlorodiphenyl	$C_{12}H_7Cl_3$	41	16.2	chloro aromatic
96	2,4,6-trichlorodiphenyl	$C_{12}H_7Cl_3$	41	17.7	chloro aromatic
97	4-chlorodiphenyl	$C_{12}H_9Cl$	41	17.5	chloro aromatic
98	chlorobenzene	C_6H_5Cl	40	10.6	chloro aromatic
99	cyclohexane	C_6H_{12}	36	7.0	cycloalkane
100	ethyl cyclohexane	C_8H_{16}	42	10.2	cycloalkane
101	isopropyl cyclohexane	C_9H_{18}	42	11.0	cycloalkane
102	methyl cyclohexane	C_7H_{14}	42	8.5	cycloalkane
103	acetone	C_3H_6O	29	6.4	ketone
104	dibutyl acetone	$C_9H_{18}O$	29	14.3	ketone
105	dipropyl acetone	$C_7H_{14}O$	29	11.1	ketone
106	ethyl-isoamyl-acetone	$C_8H_{16}O$	29	12.1	ketone
107	mesityl oxyde	$C_6H_{10}O$	29	11.4	ketone
108	methyl-butyl-acetone	$C_6H_{12}O$	29	10.3	ketone
109	methyl-ethyl-acetone	C_4H_8O	29	7.9	ketone
110	methyl-heptyl acetone	$C_9H_{18}O$	29	14.9	ketone
111	methyl-hexyl acetone	$C_8H_{16}O$	29	13.1	ketone
112	methyl-isobutyl-acetone	$C_6H_{12}O$	29	9.9	ketone
113	2-methyl thiophene	C_5H_7S	40	10.0	thiophene
114	2-methylthianaphene	C_9H_9S	40	15.8	thiophene
115	3-methyl thiophene	C_5H_7S	40	10.0	thiophene
116	3-methylthianaphene	C_9H_9S	40	15.8	thiophene
117	thianaphthene	C_8H_6S	40	14.1	thiophene
118	thiophene	C_4H_4S	40	8.0	thiophene

tive. However, there is no interaction when the atoms are a long distance from each other.

The calculated binding energy, Ecal*, can be determined from

$$\text{Ecal*} = \text{E}_{\text{ms}} - \left(\text{E}_{\text{s}} + \text{E}_{\text{m}}\right) \quad (1)$$

where E_m is the energy of an isolated gas phase molecule, E_s is the energy of the isolated surface adsorbent material, and E_{ms} is the energy of the molecule and solid surface system where the molecule is placed on the surface to represent the adsorbed state [21]. Considering the equation above to represent the final minus the initial state, the molecule has gone from being free in the gas phase to being adsorbed on the surface. The energy of adsorption is a negative energy value but the values are reported here as absolute values and in kcal/mol since these units are frequently used in molecular modeling. Desorption energies would be positive values since an input of energy is required. The equation above is equivalent to considering the energy difference, ΔE, as

$$\Delta\text{E} = \text{E}_{\text{near}} - \text{E}_{\text{far}} \quad (2)$$

with respect to the energy of the molecule adsorbed on the surface, E_{near}, and the energy of the separated and non-interacting molecule and surface, E_{far}. Therefore Ecal* = ΔE. To distinguish the experimental and calculated binding energies they are indicated as E* and Ecal*, respectively.

The experimental binding energies on a single layer graphene surface and many layer graphite surface are reported as E*(graphene) and E*(graphite), respectively. Molecular modeling values of a one layer graphene and a three layer graphite surface are indicated as Ecal*(1) and Ecal*(3), respectively. In prior work it has been shown that a three graphene layer was adequate to represent molecule-graphite interactions in molecular modeling calculations [21]. More than 90% of the vdW interaction is due to the first layer, less than 10% due to the second layer and 1% or less due to the third layer in the MM2 parameters for molecule carbon surface interactions [21]. Our interest is in predicting E*(graphene) values for organic molecules. This work considers how E*(graphene), E*(graphite), Ecal*(1), and Ecal*(3) are all intercomnected.

The relationship between the experimental E*(graphite) and calculated Ecal*(3) can be expressed as

$$\text{E*}\left(\text{graphite}\right) = \alpha\text{Ecal*}\left(3\right) \quad (3)$$

where α is the coefficient or equation multiplied by Ecal*(3) to approximate E*(graphite). This equation assumes either a simple linear relation with a fixed α or an α based on an equation to provide a connection between the experimental and model calculated values and assumes a relation that scales to zero as the values decrease. Such a relation was observed and various methods used to generate the α term or equation are discussed subsequently.

The relationship between the calculated values for the graphene one-layer and graphite three-layer model surfaces may be expressed as

$$\text{Ecal*}\left(1\right) = \beta\text{Ecal*}\left(3\right) \quad (4)$$

where β is the coefficient multiplied by Ecal*(3) to approximate Ecal*(1). This equation assumes a linear relation between the molecular modeling binding energies calculated for our graphene one layer surface model and our graphite three-layer surface model and a relation that scales to zero as the values decrease. Such a relation was observed between these calculated values and will be discussed.

We further assume that the relationship between the experimental E*(graphene) and calculated Ecal*(1) will be analogous to Equation (3) and thus can be expressed as

$$\text{E*}\left(\text{graphene}\right) = \alpha\text{Ecal*}\left(1\right). \quad (5)$$

Based on the above equations, predictions of molecule-graphene binding energies can be made by calculating Ecal*(1) and using Equation (5) or instead by calculating Ecal*(3) and using the relation below that results from combining Equations (4) and (5) to give

$$\text{E*}\left(\text{graphene}\right) = \alpha\beta\text{Ecal*}\left(3\right). \quad (6)$$

Such an approach gives a means to reasonable estimate binding energies on graphene provided Equations (3) and (4) are found to be valid.

Prior work on flat, rough, and porous surfaces has indicated that MM2 parameters may be used to calculate molecule-surface binding energies that compare well to experimental values obtained from gas-solid chromatography (GSC) in the Henry's Law region of low coverage over a range of temperatures [22-25]. With a modified model that took into account molecule-molecule nearest neighbor interactions, monolayer coverage binding energies were obtained that compared well to values obtained from thermal program desorption (TPD). For example the published E* and our calculated Ecal* associated with monolayer desorption from graphite were found to be 0.50 and 0.52, 0.72 and 0.71, 1.41 and 1.47, and 2.18 and 1.86 eV for benzene, o-dichlorobenzene, coronene, and ovalene, respectively [21].

Previously binding energies for DNA/RNA nucleobases adsorbed on single layer graphene were calculated [43]. These calculations using direct classical MM2 parameters without modification compared well to more sophisticated quantum calculations. The molecular mechanics Ecal* values were observed to be between the values from Moller-Plesset perturbation theory which

were reported to overestimate and the values from density functional theory (DFT) which were reported to underestimate molecule-surface binding energies [43].

The goal of this work is to develop a simple and effective means to estimate molecule-surface binding energy values for a variety of organic molecules adsorbed on graphene by comparisons to known molecule-graphite binding energy values.

4. Analysis and Results

Molecular mechanics MM2 calculations were performed with Scigress computer software (Fujitsu, Version 7.7.0) with the geometry optimized in mechanics using augmented MM2 parameters. The graphene model surface consisted of one layer of 702 benzene rings with no hydrogen atoms. The graphite model surface consisted of three of these layers each containing 702 rings. The layers were oriented in the form of Bernal graphite with the first layer and third layer directly aligned and the second layer offset by half a benzene ring.

To simulate the adsorption of molecules with graphite or graphene, molecules were oriented parallel to the surface and adjusted to maximize the physical interaction of molecules on the surface. The rules used for molecule placement were that first, a carbon from a methyl group of the molecule was placed above the middle of the center benzene ring in the top layer. The carbon was placed in the middle by making it equidistant from 3 alternating carbon atoms in the ring. Second, if the molecule was a cyclo or benzene containing molecules with no attached alkyl groups attached, then some carbon in the ring was selected and centered above the surface six member ring. Third the molecule was further oriented so that the more polarizable atoms were nearest the surface. The molecule was then pushed in closer than an expected optimal separation. With distances between the molecules and the surfaces of approximately 0.23 - 0.27 nm, the molecules were pushed out to the optimal distance after the molecular mechanics energy optimization calculation.

The 118 molecules listed in **Table 1** were modeled and optimized as isolated molecules in the gas phase to calculate E_m, and as described above, the molecules were then placed on a graphite model surface to calculate the E_{ms} energy. For each molecule these two values were used along with the E_s energy for the graphite three-layer model surface and Equation (1) to calculate Ecal*(3). The model-based calculated values of Ecal*(3) for 118 molecules are given in **Table 2** where they may be compared to the experimental values found in **Table 1**. The ratios of E*(Graphite)/Ecal*(3) were found to vary from 0.77 to 1.12 and these values also are given in **Table 2**.

A series of different approaches were examined to find the best means of correlation between the E*(graphite) and Ecal*(3) values. These approaches included (Method I) direct correlation of all data, (Method II) correlations of molecule subsets, (Method III) correlation of rigid and flexible subgroups, and (Method IV) correlation based on consideration of fraction of non-hydrogen atoms that are sp^3 carbon atoms.

In Method I values of E*(graphite) vs. Ecal*(3) were plotted and a linear regression through the origin determined. A graph through the origin is desirable so that the E*(graphite) and Ecal*(3) values scale to zero appropriately. The resultant linear equation (see **Figure 1**) is

$$E^*(\text{graphite}) = 0.9321\ \text{Ecal}^*(3) \tag{7}$$

with $R^2 = 0.8906$ and n = 118.

In Method II comparison, the 118 molecules were divided into 11 different functional groups that included aldehyde, alkane, alkene/alkyne, alkyl alcohol, alkyl amine, aromatic amine, benzene derivative, chlorobenzene, cycloalkane, ketone, and thiophene. E*(graphite) data versus Ecal*(3) data, were plotted for each of the 11 groups of molecules. As mentioned previously, for appropriate scaling all linear regressions were required to go through the origin. **Table 3** gives the number of data points, the slope, and the R^2 values for each group. The data points available within a group varied from a low of 4 molecules in the cycloalkane category to a high of 24 in the benzene derivative category. As shown in **Table 3**, the R^2 values varied from a low of 0.8726 for cycloalkane (n = 4) to a high of 0.9756 for alkene/alkyne (n = 7). The slopes varied from a low of 0.8729 for alkane to 1.0312 for chloroaromatic. Recall that for the combined set of all the molecules (n = 118) the R^2 value was 0.8906. All the subset groups have a higher R^2 except for the cycloalkane at 0.8726.

Method III was based on the observation that the linear regressions of aromatic amine, benzene derivative, chloroaromatic, and thiophene have slopes of 1.0169, 0.9633, 1.0312, and 0.9936, respectively. This indicates that the computed interaction energies, Ecal*(3) values that without modification agreed well with the experimental values of E*(graphite). So if a molecule had a benzene or other flat ring structure such as the thiophene, the molecule was classified as "rigid." Therefore the aromatic amine, benzene derivative, chloroaromatic, and thiophene groups were combined and considered together as the rigid group. When all these data (n = 60) are plotted together, the correlating equation is

$$E^*(\text{graphite}) = 0.9918\ \text{Ecal}^*(3) \tag{8}$$

with ($R^2 = 0.9130$).

As shown in **Table 3**, the data for the remaining groups of molecules: aldehyde, alkane, alkene/alkyne, alkyl alcohol, alkyl amine cycloalkane, and ketone had slopes that varied from 0.8288 for alkyl amine to 0.9057

Table 2. Molecule numbers with the calculated binding energy values for graphite Ecal*(3), modified graphite values Ecal*(3)-mod, ratio of experimental to calculated graphite binding energies E*/Ecal*(3), ratio of experimental to modified calculated graphite binding energies E*/Ecal*(3)-mod, calculated one layer graphene values Ecal*(1), and predicted values for graphene binding energies.

Number	Ecal*(3) kcal/mol	Ecal*(3)-mod kcal/mol	E*/Ecal*(3)	E*/Ecal*(3)-mod	Ecal*(1) kcal/mol	E*(graphene)-predict kcal/mol
1	8.6506	7.7828	0.86	0.95	8.1015	7.3
2	11.1165	9.742	0.93	1.06	10.4058	9.1
3	14.9574	12.9141	0.90	1.04	13.9463	12.0
4	8.2166	8.0632	1.06	1.08	7.6482	7.5
5	7.3589	6.6207	0.98	1.09	7.0007	6.3
6	8.8775	7.8661	0.98	1.11	8.3008	7.4
7	16.5201	14.1884	0.85	0.99	15.4480	13.3
8	6.8425	6.2958	0.98	1.06	6.4034	5.9
9	10.3547	9.175	0.85	0.96	9.7028	8.6
10	4.7612	3.8948	0.90	1.10	4.4724	3.7
11	8.4293	6.8954	0.81	0.99	7.9153	6.5
12	19.6667	16.0879	0.82	1.00	18.4730	18.8
13	14.0388	11.4841	0.83	1.02	13.2000	10.8
14	12.0938	9.8931	0.85	1.04	11.3530	10.9
15	17.7549	14.524	0.82	1.01	16.6638	13.6
16	15.7817	12.9099	0.84	1.03	14.8105	12.1
17	6.6601	5.4481	0.80	0.97	6.2488	5.1
18	7.311	6.7268	0.92	1.00	6.8623	6.3
19	18.2374	15.6633	0.84	0.98	16.8021	14.5
20	12.5233	10.9748	0.89	1.02	11.6826	10.2
21	10.7325	9.5098	0.93	1.05	10.0684	10.3
22	16.2582	14.0372	0.87	1.01	15.2171	15.2
23	14.4672	12.5729	0.89	1.03	13.5386	11.8
24	6.9502	6.7495	0.92	0.95	6.5403	6.4
25	15.1773	12.8027	0.82	0.97	14.2459	12.0
26	13.4105	11.3612	0.81	0.96	12.5882	10.7
27	10.2173	8.7056	0.83	0.98	9.6006	8.2
28	8.2506	7.0861	0.91	1.06	7.7106	6.6
29	7.163	6.2251	0.94	1.08	6.7163	5.8
30	11.5711	9.8592	0.82	0.96	10.8568	9.3
31	9.8345	8.4464	0.84	0.98	9.2276	7.9
32	7.8316	6.8061	0.87	1.00	7.3479	6.4
33	10.4037	8.8645	0.83	0.97	9.7412	8.3
34	7.7058	6.6182	0.99	1.15	7.2012	6.2
35	8.4669	7.2142	0.92	1.08	7.9534	6.8
36	7.6704	6.5878	0.94	1.09	7.2051	6.2
37	20.5656	17.2049	0.77	0.92	19.3175	16.2

Continued

38	16.9265	14.2303	0.79	0.93	15.8909	14.9
39	13.8254	11.6231	0.88	1.05	12.9545	12.3
40	13.1701	11.1576	0.78	0.92	12.3575	11.9
41	24.9434	20.7226	0.85	1.03	23.4343	19.5
42	19.6055	16.3457	0.88	1.06	18.4211	15.1
43	10.54	8.9294	0.83	0.97	9.8632	8.1
44	10.4035	9.2183	0.83	0.93	9.7249	8.6
45	9.9188	8.2979	1.05	1.25	9.3384	7.8
46	7.7967	7.9695	1.03	1.00	7.2819	7.4
47	18.0297	17.8159	0.97	0.98	16.8329	16.6
48	10.1525	8.4934	1.05	1.26	9.5514	8.0
49	17.4376	17.1769	0.97	0.98	16.2713	16.0
50	15.5252	15.5524	1.03	1.03	14.4886	14.5
51	17.3498	17.7343	1.00	0.98	16.1790	16.5
52	12.354	12.1234	1.04	1.06	11.4931	11.3
53	11.2788	11.0171	1.12	1.14	10.2624	9.1
54	12.2977	12.5703	0.94	0.92	11.4819	11.7
55	10.8717	11.1127	1.09	1.07	10.0317	8.9
56	17.3573	17.4199	1.01	1.01	16.2012	16.3
57	19.2333	19.6596	1.10	1.07	17.8932	18.3
58	13.6384	13.9407	1.10	1.08	12.7200	13.0
59	14.3381	14.29	0.93	0.93	13.4207	13.4
60	13.4991	13.4538	1.01	1.01	12.5911	12.5
61	15.4251	14.6219	1.07	1.13	14.4485	14.7
62	14.6248	14.2855	1.05	1.07	13.6487	13.3
63	14.2315	14.1838	0.93	0.94	13.2930	13.2
64	14.4434	14.395	0.93	0.93	13.4916	13.4
65	8.3784	8.5641	1.04	1.02	7.8201	8.0
66	8.9317	9.1297	1.04	1.02	8.3523	8.5
67	16.3601	16.4191	0.97	0.96	15.2564	15.3
68	16.9358	15.9283	0.93	0.99	15.8278	13.4
69	17.0702	16.287	0.85	0.89	16.1040	16.3
70	15.5725	14.858	0.92	0.96	14.5969	13.6
71	18.2023	17.9864	1.00	1.01	16.9797	14.4
72	16.2701	16.3288	1.04	1.04	15.1739	13.1
73	9.576	9.7882	0.93	0.91	8.8834	9.1
74	16.6829	16.7431	1.02	1.02	15.5687	15.6
75	19.6911	20.1275	1.05	1.02	18.3850	15.4
76	15.4355	15.7776	1.06	1.03	14.3828	14.4
77	12.1126	11.7629	0.92	0.95	11.2379	10.5

Continued

78	18.2586	18.3766	1.06	1.06	17.0269	17.1
79	20.2064	18.5918	0.93	1.01	18.9263	17.4
80	11.4603	10.9345	1.00	1.05	10.6949	10.2
81	13.6196	13.2264	0.93	0.95	12.7310	13.0
82	17.5189	16.2816	0.83	0.90	16.3308	15.2
83	15.5873	14.66	0.87	0.93	14.5106	13.9
84	13.8437	13.2085	0.92	0.97	12.8623	10.9
85	14.6034	14.9271	1.02	1.00	13.6477	14.0
86	13.1729	12.7926	0.96	0.98	12.2962	10.5
87	13.5546	13.1633	0.93	0.96	12.6671	12.3
88	22.6612	23.1635	1.00	0.98	21.1151	21.6
89	18.2592	16.9696	0.95	1.03	17.1053	15.9
90	11.5674	11.4864	0.89	0.90	10.8043	10.7
91	12.9318	13.2184	0.96	0.94	12.0376	12.3
92	12.8689	13.1541	0.99	0.97	11.9701	12.2
93	14.8622	15.1916	1.06	1.04	13.8765	14.2
94	15.2383	15.576	1.06	1.04	14.3751	14.7
95	15.4103	15.7518	1.05	1.03	14.4006	13.7
96	16.3088	16.6703	1.09	1.06	15.2360	15.6
97	17.1266	17.5062	1.02	1.00	15.9001	15.4
98	11.2641	11.5138	0.94	0.92	10.4851	10.0
99	8.7455	7.1541	0.80	0.98	8.2032	6.7
100	11.8776	9.7162	0.86	1.05	11.1466	9.1
101	11.8508	9.6943	0.93	1.13	11.1610	9.1
102	10.5161	8.6025	0.81	0.99	9.8764	8.4
103	7.0548	6.4911	0.91	0.99	6.6022	6.1
104	17.7988	15.2866	0.80	0.94	16.6893	14.3
105	14.0043	12.1706	0.79	0.91	13.1325	11.4
106	14.6858	12.6796	0.82	0.95	13.8034	11.9
107	12.0338	11.2477	0.95	1.01	11.2562	9.3
108	12.4057	10.8718	0.83	0.95	11.6537	10.2
109	8.7048	7.8315	0.91	1.01	8.1405	7.3
110	17.9867	15.448	0.83	0.96	16.8834	16.8
111	16.1562	13.9491	0.81	0.94	15.1430	13.1
112	11.1266	9.7508	0.89	1.02	10.4099	10.7
113	10.7257	10.5985	0.93	0.94	9.9975	9.9
114	15.7348	15.7623	1.00	1.00	14.6754	14.7
115	10.604	10.4782	0.94	0.95	9.8864	9.8
116	15.4225	15.4495	1.02	1.02	14.3652	14.7
117	13.65	13.9525	1.03	1.01	12.7079	12.4
118	8.5846	8.7749	0.93	0.91	7.9981	8.2

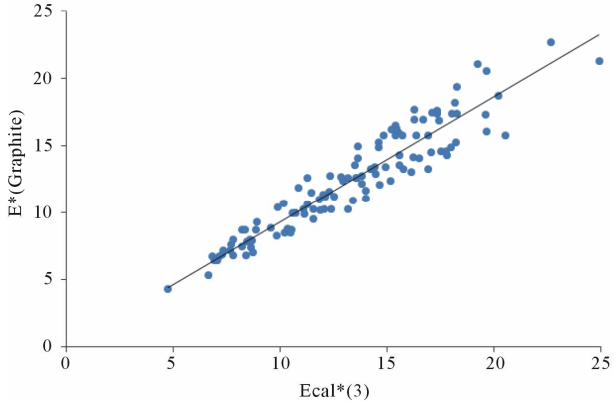

Figure 1. Experimental organic molecule-graphitic surface binding energies versus three layer calculated binding energies for 118 adsorbate molecules gave a linear regression of E*(graphite) = 0.9321 Ecal*(3) with (R^2 = 0.8906).

Table 3. Number of data points, the slope, and the R^2 values for each group. The data points available within a group varied from a low of 4 molecules in the cycloalkane category to a high of 24 in the benzene derivative category. R^2 values varied from a low of 0.8726 for cycloalkane to a high of 0.9756 for alkene/alkyne. The slopes varied from a low of 0.8729 for alkane to 1.0312 for chloroaromatic.

Functional Group	Parameters		n
	Slope	R^2	
aldehyde	0.9057	0.9308	9
alkane	0.8291	0.9971	8
alkene/alkyne	0.8751	0.9756	7
alkyl alcohol	0.8564	0.9043	13
alkyl amine	0.8288	0.96	7
ketone	0.8362	0.9421	10
cycloalkane	0.8581	0.8726	4
aromatic amine	1.0169	0.9394	22
benzene	0.9633	0.8971	24
chloroaromatic	1.0312	0.9257	8
thiophene	0.9936	0.9728	6

for aldehyde and were grouped together in what we considered as the "flexible" category. The flexible molecules lacked a flat ring structure in the molecule and so had potentially more conformational flexibility. The average of the slopes in **Table 3** for these seven groups was 0.8556 with a 0.0280 standard deviation. When all these "flexible" data (n = 58) are plotted together, the correlating equation is

$$E^*(\text{graphite}) = 0.8500\ \text{Ecal}^*(3) \qquad (9)$$

with (R^2 = 0.9621).

While these R^2 values of 0.9130 for the rigid and 0.9621 for the flexible molecules are better than the R^2 of 0.8906 for all the molecule together, a still better correlation is needed to be able to effectively use Ecal*(3) values to predict E*(graphite). From the considerations above, it is clear that the calculated values are too high for the "flexible" structures since as shown in **Figure 2** the Ecal*(3) values must be multiplied by on average 0.85 to bring their values down to agreement with the E*(graphite) experimental values. However, there is more variation within individual molecules than simply placing into these two groups.

To reconcile the differences observed for the "rigid" and "flexible" molecules and to have one common equation and one correlation for all the molecules, a different approach was needed. We observed that the MM2 vdW parameters for the sp^3 carbon atoms were overestimating their carbon surface interactions and hence could be correlated only by using about 85% of their estimated binding energy values. The flexible molecule category was dominated by tetrahedral bonded carbons which we label below as C-sp^3 atoms. However, the trigonal planar sp^2 carbons dominated the so called rigid molecules had MM2 vdW parameters that matched well with the experimental interaction energies and hence had slopes close to one. In examining the individual molecules we were able to observe variations depending on the number of C-sp^3 atoms and C-sp^2 and other atoms. These observations led to the next approach.

In Method IV for every molecule all non-hydrogen atoms were counted and placed into one of two categories. The atom was either a sp^3 hybridized carbon or not. The non sp^3 carbon atoms included sp^2 trigonal planar bonding carbon atoms, sp linear bonding carbon atoms, and all other atoms such as oxygen, nitrogen, sulfur. All hydrogen atoms were excluded from the counting process. So the relations may be summarized as

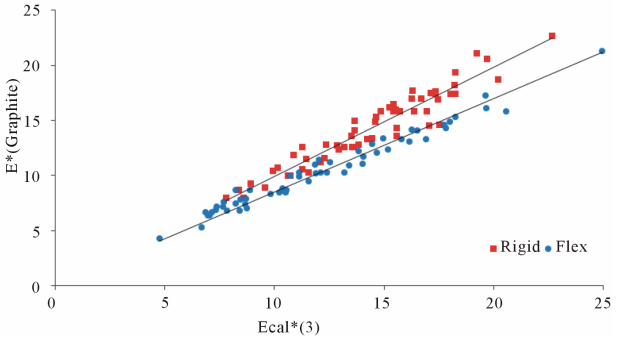

Figure 2. Experimental organic molecule-graphitic surface binding energies versus three layer calculated binding energies for rigid (n = 60) and flexible (n = 58) adsorbate molecules gave linear regressions of E*(graphite) = 0.9918 Ecal*(3) with R^2 = 0.9130 and E*(graphite) = 0.8500 Ecal*(3) with R^2 = 0.9621, respectively.

$$n_{total} = n_{C\text{-}sp3} + n_{other} \quad (10)$$

$$f_{C\text{-}sp3} = n_{C\text{-}sp3} / n_{total} \quad (11)$$

$$f_{other} = n_{other} / n_{total} \quad (12)$$

$$1 = f_{C\text{-}sp3} + f_{other} \quad (13)$$

where n_{total} is the total number of nonhydrogen atoms, $n_{C\text{-}sp3}$ is the number of sp^3 carbon atoms, n_{other} is the number of all other nonhydrogen and non sp^3 carbon atoms, $f_{C\text{-}sp3\text{-}c}$ is the fraction of sp^3 carbon atoms, and f_{other} is the fraction of all other nonhydrogen atoms.

Using the above relations then the Equation (3) may be written as

$$E^*(\text{graphite}) = \left(c_{C\text{-}sp3}\ f_{C\text{-}sp3} + c_{other}\ f_{other}\right)\ Ecal^*(3) \quad (14)$$

$c_{C\text{-}sp3}$ and c_{other} are the best fit coefficients multiplied by the fraction of sp^3 carbon atoms and fraction of other non-hydrogen atoms, respectively. The α term in Equation (3) is now represented as α = ($c_{C\text{-}sp3}$ $f_{C\text{-}sp3}$ + c_{other} f_{other}). The $c_{C\text{-}sp3}$ and c_{other} were derived from multilinear regression calculation using E*(graphite) and Ecal*(3) values in **Table 1** along with $f_{C\text{-}sp3}$ and f_{other} values for each of the 118 molecules. The best fit coefficients for $c_{sp3\text{-}C}$ was found to be 0.8180 and for c_{other} was found to be 1.0221.

The originally calculated Ecal*(3) for each of the 118 molecules could then be modified by the equation for α in Equation (14) and are given in **Table 2**. These modified values are indicated as Ecal*(3)-modified. For example, consider the molecule 1,2,3,5-tetramethylbenzene that consist of 4 sp^3 carbon atoms and 6 sp^2 carbon atoms. The fractions are $f_{C\text{-}sp3}$ = 0.4000 and f_{other} = 0.6000. Using the best fit values of the fractions $c_{sp3\text{-}C}$ gives [(0.8180) (0.4000) + (1.0221) (0.6000)] 16.9358 kcal/mol = [0.9405] [16.9358] = 15.9274 or 15.9 kcal/mol. Clearly 15.9 is much better estimate of the reported experimental binding energy of 15.8 kcal/mol.

Figure 3 shows a plot of E*(Graphite) versus Ecal*(3)-modified where

$$Ecal^*(3)\text{-modified} = \left(0.8180\ f_{C\text{-}sp3} + 1.0221\ f_{other}\right)\ Ecal^*(3) \quad (15)$$

The linear regression for E*(graphite) versus Ecal*(3)-modified (n = 118) gave a slope of 1.0000 and (R^2 = 0.9647). While still using the standard MM2 parameters this approach provides a fairly simple modification that provides reasonable estimates of E*(graphite). A comparison of **Figures 1** and **3** shows a change of R^2 from 0.8906 to 0.9647 indicating a significant improvement in the correlation.

Next, it was necessary to determine values of Ecal*(1). A molecule must have same placement and orientation for accurate comparison. The only part that should be different was the number of layers for the surface. To convert graphite to graphene, the second and third layers were removed from molecules already placed on the graphite model using the procedure previously described. The E_{ms} was recalculated for each molecule after MM2 optimization and then used with E_m values and an E_s(graphene) calculated value to find Ecal*(1) using Equation (1). The average ratio of Ecal*(1)/Ecal*(3) for the 118 molecules gave an average and standard deviation of 0.9350 ± 0.004. **Figure 4** shows a plot of Ecal*(1) versus Ecal*(3) and the slope based on a linear regression was 0.9349 with (R^2 = 0.9998). The results indicated the calculated binding energy of a molecule on graphene is consistently 93.5% of the calculated value on graphite. Thus, the β from Equation (4) is determined to be 0.935 and may the relation may be expressed as

$$Ecal^*(1) = 0.935\ Ecal^*(3) \quad (16)$$

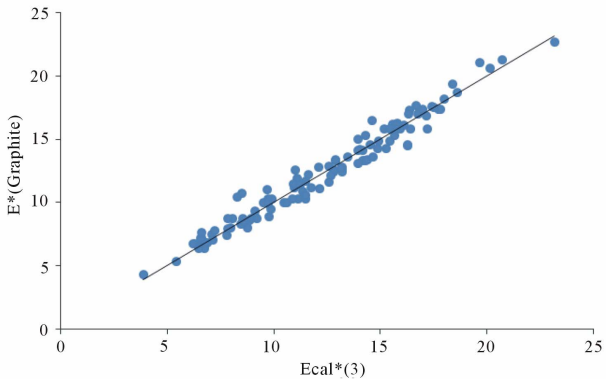

Figure 3. Experimental organic molecule-graphitic surface binding energies versus modified three layer calculated binding energies for 118 adsorbate molecules gave a linear regression of E*(graphite) = 1.0000 Ecal*(3)-modified (n =118) with (R^2 = 0.9647).

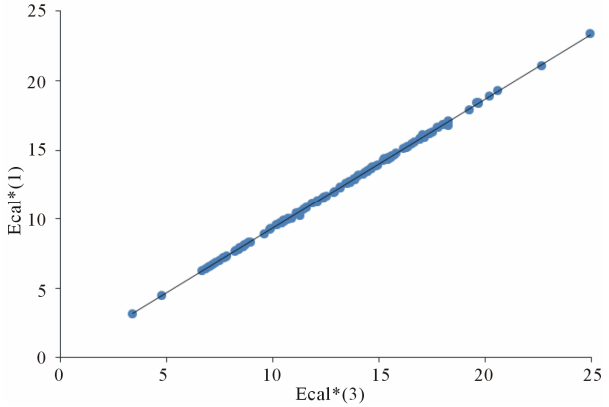

Figure 4. Plot of Ecal*(1) modeling binding energy on graphene versus Ecal*(3) modeling binding energies on graphite for 118 organic adsorbate molecules gave a linear regression with a slope of 0.9349 and (R^2 = 0.9998).

So we propose that using MM2 parameters for a molecule in optimized geometry and then placed on a three layer graphite surface can give a reasonable estimate of the graphene binding energy using our Equation (6) expressed after combining Equations (14) and (15) to give

$$E^*(\text{graphene}) = 0.935\left[0.8180\, f_{C\text{-}sp3} + 1.0221\, f_{other}\right] Ecal^*(3) \quad (17)$$

Or more directly if a molecule is placed on a single layer model graphene surface, a reasonable estimate of the expected molecule-graphene interaction or binding energy is obtained from

$$E^*(\text{graphene}) = \left[0.8180\, f_{C\text{-}sp3} + 1.0221\, f_{other}\right] Ecal^*(1) \quad (18)$$

It is assumed that the graphite correction also can be applied to graphene. This assumption is reasonable considering a single carbon layer accounts for 93.5% of the MM2 graphite binding energies for the 118 molecules considered. The c_{Csp3} and c_{other} above are taken directly from Equation (15). The α in Equation (3) is now represented from the above as $\alpha = (c_{C\text{-}sp3}\, f_{C\text{-}sp3} + c_{other}\, f_{other})$.

5. Discussion

The binding energy of an adsorbate molecule on an adsorbent surface can be affected by molecule size, molecule orientation, and the nature of surface. For organic molecules adsorbed on graphitic surfaces, van der Waals forces tend to dominate the physical adsorption. Larger more polarizable atoms tend to increase vdW forces increase the binding energy. For example, comparing molecules M91 1,3-dichlorobenzene and M73 benzene, one observes E* values of 12.4 and 8.9 kcal/mol, respectively. More atoms in a molecule increases the vdW forces. For example, comparing molecules M12 decane and M11 butane, one observes E* values of 16.1 and 6.8 kcal/mol, respectively. Different orientations of the molecule and different conformations can also affect the binding energy. Orientations of molecules were selected to have the maximum contact with the surface. Since our focus was to find the lowest energy for a molecule adsorbed on a surface, we chose the most polarizable atom facing the surface as previously described because the vdW is stronger with more polarizable atoms near the surface and a flat orientation to put as much of the molecule on the surface as possible.

The approach illustrated in **Table 3** was to divide the experimental values into one of nine subgroups based on the molecular structure of the adsorbate. With the exception of the cycloalkane group that only had four molecules and $R^2 = 0.8726$, all the remaining R^2 values were better than the set of all 118 molecules with $R^2 = 0.8906$. The R^2 for the eight other groups ranged from 0.8971 up to 0.9971. However it was desirable to have one general equation that would allow calculation of Ecal* for whatever molecule was selected without regard to functional group.

As shown in **Table 2**, our coefficients and the equation do not make our Ecal* values match with E* exactly. However, our modification provides a reasonable approach to interpret the over-calculated values for the atoms with sp^3 hybridizations and improves the match of calculated and experimental values. Using the values of the E*/Ecal*(3) ratios gives an average of 0.93 and a 0.09 standard deviation. Using the values of the E*/Ecal*(3)-modified ratios gives an average of 1.01 and 0.07 standard deviation. This modification was necessary to successfully predict the binding energy. **Figure 1** shows the E* versus Ecal* plots somewhat scattered with R^2 of 0.8906 and a slope of 0.9321. However, **Figure 3** shows E* versus Ecal*(3)-modified with a slope of 1.0000 and R^2 of 0.9647. So Equation (15) provides an effective method to estimate E*(graphite) by modifying computed values of Ecal*(3). There is a regular relation between Ecal*(1) and Ecal*(3) with the Ecal*(1) values being 93.5% of the Ecal*(3) values as shown in **Figure 4** and in **Table 2**.

Our initial adjustment for the scatter in **Figure 1** was to place molecules in categories of rigid (ring containing) or flexible (no ring) as illustrated in **Table 3** based on the slopes that were near one for aromatic amine, benzene derivatives, chloroaromatic, and thiophene groups but clearly less than one for the remaining seven groups. While this division into two categories led to improved correlation coefficients with R^2 equal to 0.9621 and 0.9130 for the flexible and rigid, respectively the cause of this difference was based on the overestimate of vdW forces between the surface carbon atoms and sp^3 carbon atoms. For instance, **Table 2** shows the ratio of E* (graphite)/Ecal*(3) is 0.87 for n-butyl benzene (M83) but for naphthalene (M85) this ratio is 1.02 meaning the calculated and experimental are in close agreement. Both molecules have same number of carbons but the Ecal* is about 15% too large due to the calculated vdW energy being too high.

Since this overestimation occurs in a regular pattern we were able to adjust the Ecal* simply based on the fraction of nonhydrogen atoms that were sp^3 carbon atoms. This adjustment was accomplished by Equation (15) where the fraction of sp^3 carbons is multiplied by 0.8180 Ecal* to give its E* contribution to E* and the fraction of all other nonhydrogen atoms is multiplied by 1.0221 Ecal* to give its contribution to E*. We see that on average sp^3 carbons have a value that is too high and all other nonhydrogen atoms have values that are on average

slightly low.

To test the application of our approach a molecule not in the original set of 118 molecules was selected for estimation of E*(graphite) and E*(graphene). C. Thierfelder *et al.* reported calculated binding energies of methane on graphene with five different methods [44]. They used a reported experimental value of methane on graphite in the range of 0.12 - 0.14 eV. They also made an assumption that the binding energy of methane on graphene should be about 0.01 eV less than on graphite so their estimated binding energy value for methane on graphite was E*(graphite) = 0.12 to 0.14 eV and on graphene they estimated E*(graphene) = 0.11 to 0.13 eV. Our estimated energy for Ecal*(3) for methane was 3.40 kcal/mol and Ecal*(3)-modified was 2.8 kcal/mol (0.12 eV) and the predicted Ecal*(graphite) was 2.6 kcal/mol (0.11 eV). So our estimated binding energies of E*(graphite) = 0.12 eV and E*(graphene) = 0.11 eV agree with well their suggested values.

6. Conclusions

The weakness of noncovalent vdW interactions presents a general challenge for more exact quantum mechanical methods and density functional theory (DFT) calculations as indicated by a comparison of 40 density functionals with noncovalent interaction energies [45,46]. DFT results have been reported to underestimate vdW interactions [47]. However, Moller-Plesset perturbation theory (MP2) has been reported to overestimate the binding energies [48]. The basis set used to model a molecule and a dimer cluster (benzene-coronene for example) can greatly affect the interaction energy. This error is known as the basis set superposition error (BSSE). For benzene-coronene quantum calculations where coronene can be used to represent a graphene surface the MP2 results had to be modified by a counterpoise correction of about 40% [48]. Tauer and Sherrill examined π-π interactions for benzene dimers and trimmers and found that MP2 calculations with small basis sets tended to have cancelling errors. By allowing these errors to offset each other they were able to find interaction energies close, few tenths of kcal/mol, of a complete basis set couple cluster CCSD(T) limit [49]. Because of these computational challenges, for ease of use, for representations of larger surface areas or multiple molecules, and for simpler and quicker calculations it can be useful to make estimates based on molecular mechanics and the approach outlined in this work.

We used augmented MM2 parameters and classical molecular modeling to predict molecule-graphene binding energies of 118 organic molecules. Our results suggest that this method can provide useful estimates of experimental values that may otherwise be difficult to obtain. In prior work MM2 parameters and molecular mechanics calculations have been used to estimate molecule surface interaction energies on flat, rough, and porous carbon surfaces [22-25,43].

The calculated binding energies for a molecule on the single layer graphene model were consistently found to be 93.5% of the value for the same molecule on the three-layer graphite model. This is in agreement with prior work for nucleobases on graphene and graphite that showed going from 1 to 3 layers increased binding energy by 8% to 10% [43]. The MM2 calculations for these binding energies are dominated by vdW forces and these have been observed to give reasonable correlations when a standard 0.9 nm cutoff value was used. One implication for future sensor devices based on adsorption due to dispersive forces on bilayer graphene is that the interaction energy for a bilayer should be very close, within a few percent, to the value for graphite.

Although the MM2 parameters were not optimized for adsorption energy calculations, the values obtained for vdW dominated adsorption on carbon give good correlations with experimental. It was observed that calculated Ecal* values had to be corrected to better agree with the experimental E* for the set of 118 organic molecules used. The calculated binding energy was corrected with simple modification using coefficients that reduced the energy contribution from all sp^3 carbon atoms by multiply the fraction of these atoms by 0.818 and the remaining carbon and heteroatoms (hydrogen atoms were not included in determining these fractions) were almost unchanged being multiplied by 1.022, respectively.

The direct MM2 results gave the ratio of E*/Ecal*(3) as 0.93 (n = 118) with a standard deviation of 0.09. The modified MM2 results gave the ratio of E*/Ecal*(3)-mod as 1.01 (n = 118) with a standard deviation of 0.07. So the direct MM2 model based binding energies were on average larger than the experimental values by about 7.5% (1/0.93 = 1.075), but after the modification described previously and given in Equation (15), the average of all 118 values was within about one percent. Most calculated values were within 7% of the corresponding experimental ones (see **Table 2**). The slope of E* versus Ecal*(3)-mod was 1.00 with $R^2 = 0.965$ as shown in **Figure 3**.

The modification of the Ecal*(3) calculated values should apply to the graphene also so the Ecal*(3)-mod could be multiplied by 0.935 as shown in Equation (16) to find E*(graphene). Or more directly Ecal*(1) can be converted to E*(gaphene) using Equation (17). In other words, a molecule's interaction energy can be calculated on a three layer model or a one layer model and effectively converted to a reasonable estimate of the expected experimental interaction energy on single layer graphene surface, E*(graphene). Using our data set correlations and extending it to a molecule not included in the origin-

nal set of 118 allowed us to test this method. Binding energies of 0.12 and 0.11 eV were obtained for methane and these compared well to published experimental and estimated values for graphite and graphene, respectively.

Simpler non quantum mechanical calculations based on classical molecular mechanics continue to be of use to estimate molecule-surface binding energies based on weaker dispersion forces. This molecular mechanics approach does not provide any electronic details but it is a useful, computationally simple approach to study molecule interactions on carbon surfaces and should be helpful to predict how strongly various molecules may be held on future single layer graphene or bilayer graphene sensor detection devices. This approach may also be useful to predict interactions in other possible applications such as surface self assembly, molecular separations, or graphene-molecule storage and delivery devices.

7. Acknowledgements

We gratefully acknowledge the support provided by the Grote Chemistry Fund and the Wheeler Odor Research Center at the University of Tennessee at Chattanooga.

REFERENCES

[1] S. W. Pati, T. Enoki and C. N. Rao, "Graphene and Its Fascinating Attributes," World Scientific, Singapore, 2011.

[2] W. Choi and J. Lee, "Graphene: Synthesis and Applications," CRC Press, Boca Raton, 2012.

[3] Royal Swedish Academy of Sciences, "Scientific Background on the Nobel Prize in Physics 2010 GRAPHENE," 2010. http://www.nobelprize.org/nobel_prizes/physics/laureates/2010/advancedphysicsprize2010.pdf

[4] P. T. Araujo, M. Terrones and M. S. Dresselhaus, "Defects and Impurities in Graphene-Like Materials," *Materials Today*, Vol. 15, No. 3, 2012, pp. 98-109. doi:10.1016/S1369-7021(12)70045-7

[5] W. Choi, I. Lahiri, R. Seelaboyina and Y. S. Kang, "Synthesis of Graphene and Its Applications: A Review," *Critical Reviews in Solid State Materials Sciences*, Vol. 35, No. 1, 2010, pp. 52-71. doi:10.1080/10408430903505036

[6] H. J. Yoon, D. H. Jun, J. H. Yang, Z. Zhou, S. S. Yang and M. M.-C. Chen, "Carbon Dioxide Gas Sensor Using a Graphene Sheet," *Sensors and Actuators B*: *Chemical*, Vol. 157, No. 1, 2011, pp. 310-313. doi:10.1016/j.snb.2011.03.035

[7] Y. Zou, F. Li, Z. H. Zhu, M. W. Zhao, X. G. Xu and X. Y. Su, "An *ab Initio* Study on Gas Sensing Properties of Graphene and Si-Doped Graphene," *European Physical Journal B*, Vol. 81, No. 4, 2011, pp. 475-479. doi:10.1140/epjb/e2011-20225-8

[8] O. Leenaerts, B. Partoens and F. M. Peeters, "Adsorption of H_2O, NH_3, CO, NO_2, and NO on Graphene: A First-Principles Study," *Physical Review B*, Vol. 77, No. 12, 2008, Article ID: 125416. doi:0.1103/PhysRevB.77.125416

[9] M. Gautam and A. H. Jayatissa, "Adsorption Kinetics of Ammonia Sensing by Graphene Films Decorated with Platinum Nanoparticles," *Journal of Applied Physics*, Vol. 111, No. 9, 2012, Article ID: 094317. doi:10.1063/1.4714552

[10] Y. Ren, C. Zhu, W. Cai, H. Li, H. Ji, I. Kholmanov, Y. Wu, R. D. Piner and R. S. Ruoff, "Detection of Sulfur Dioxide Gas with Graphene Field Effect Transistor," *Applied Physics Letters*, Vol. 100, No. 16, 2012, Article ID: 163114. doi:10.1063/1.4704803

[11] M. G. Chung, D. H. Kim, H. M. Lee, T. Kim, J. H. Choi, D. K. Seo, J.-B. Yoo, S.-H. Hong, T. J. Kang and Y. H. Kim, "Highly Sensitive NO_2 Gas Sensor Based on Ozone Treated Graphene," *Sensors and Actuators B*: *Chemical*, Vol. 166-167, 2012, pp. 172-176. doi:10.1016/j.snb.2012.02.036

[12] S. Mao, S. Cui, G. Lu, K. Yu, Z. Wen and J. Chen, "Tuning Gas-Sensing Properties of Reduced Graphene Oxide Using Tin Oxide Nanocrystals," *Journal of Materials Chemistry*, Vol. 22, 2012, pp. 11009-11013. doi:10.1039/c2jm30378g

[13] H. Zhang, A. Kulkarni, H. Kim, D. Woo, Y.-J. Kim, B. H. Hong, J.-B. Choi and T. Kim, "Detection of Acetone Vapor Using Graphene on Polymer Optical Fiber," *Journal of Nanoscience and Nanotechnology*, Vol. 11, No. 7, 2011, pp. 5939-5943. doi:10.1166/jnn.2011.4408

[14] T. V. Cuong, V. H. Pham, J. S. Chung, E. W. Shin, D. H. Yoo, S. H. Hahn, J. S. Huh, G. H. Rue, E. J. Kim, S. H. Hur and P. A. Kohl, "Solution-Processes ZnO-Chemically Converted Graphene Gas Sensor," *Materials Letters*, Vol. 64, No. 22, 2010, pp. 2479-2482. doi:10.1016/j.matlet.2010.08.027

[15] J. L. Johnson, A. Behnam, S. J. Pearton and A. Ural, "Hydrogen Sensing Using Pd-Functionalized Multi-Layer Graphene Nanoribbon Networks," *Advanced Materials*, Vol. 22, No. 43, 2010, pp. 4877-4880. doi:10.1002/adma.201001798

[16] W. Wu, Z. Liu, L. A. Jauregui, Q. Yu, R. Pillai, H. Cao, J. Bao, Y. P. Chen and S.-S. Pei, "Wafer-Scale Synthesis of Graphene by Chemical Vapor Deposition and Its Application in Hydrogen Sensing," *Sensors and Actuators B*: *Chemical*, Vol. 150, No. 1, 2010, pp. 296-300. doi:0.1016/j.snb.2010.06.070

[17] H. Song, L. Zhang, C. He, Y. Qu, Y. Tian and Y. Lv, "Graphene Sheets Decorated with SnO_2 NanoParticles: *In Situ* Synthesis and Highly Efficient Materials for Cataluminescence Gas Sensors," *Journal of Materials Chemistry*, Vol. 21, No. 16, 2011, pp. 5972-5977. doi:10.1039/c0jm04331a

[18] A. Shimizu and K. Fujii, "Thin Film Gas Sensor," Japan Kokai Tokyo Koho, 2011, JP 2011169634 A 20110901.

[19] G. Lu, S. Park, K. Yu, R. S. Ruoff, L. E. Ocola, D. Rosenmann and J. Chen, "Toward Practical Gas Sensing with Highly Reduced Graphene Oxide: A New Signal Processing Method to Circumvent Run-to-Run and Device-to-Device Variations," *ACS Nano*, Vol. 5, No. 2, 2011, pp. 1154-1164. doi:10.1021/nn102803q

[20] G. Lu, L. E. Ocola and J. Chen, "Gas Detection Using Low-Temperature Reduced Graphene Oxide Sheets," *Applied Physics Letters*, Vol. 94, No. 8, 2009, Article ID: 083111. doi:10.1063/1.3086896

[21] T. R. Rybolt, C. E. Wells, C. R. Sisson, C. B. Black and K. A. Ziegler, "Evaluation of Molecular Mechanics Calculated Binding Energies for Isolated and Monolayer Organic Molecules on Graphite," *Journal of Colloid and Interface Science*, Vol. 314, No. 2, 2007, pp. 434-445. doi:10.1016/j.jcis.2007.05.083

[22] T. R. Rybolt, K. A. Ziegler, H. E. Thomas, J. L. Boyd and M. E. Ridgeway, "Adsorption Energies for a Nanoporous Carbon from Gas-Solid Chromatography and Molecular Mechanics," *Journal of Colloid and Interface Science*, Vol. 296, No. 1, 2006, pp. 41-50. doi:10.1016/j.jcis.2005.08.057

[23] T. R. Rybolt and R. A. Hansel, "Determining Molecule-Carbon Surface Adsorption Energies Using Molecular Mechanics and Graphene Nanostructures," *Journal of Colloid and Interface Science*, Vol. 300, No. 2, 2006, pp. 805-808. doi:10.1016/j.jcis.2006.04.057

[24] T. R. Rybolt, C. E. Wells, H. E. Thomas, C. M. Goodwin, J. L. Blakely and J. D. Turner, "Binding Energies for Alkane Molecules on a Carbon Surface from Gas-Solid Chromatography and Molecular Mechanics," *Journal of Colloid and Interface Science*, Vol. 325, No. 1, 2008, pp. 282-286. doi:10.1016/j.jcis.2008.06.043

[25] T. R. Rybolt, K. T. Bivona, H. E. Thomas and C. M. O'Dell, "Comparison of Gas-Solid Chromatography and MM2 Force Field Molecular Binding Energies for Greenhouse Gases on a Carbonaceous Surface," *Journal of Colloid and Interface Science*, Vol. 338, No. 1, 2009, pp. 287-292. doi:10.1016/j.jcis.2009.06.001

[26] N. L. Allinger, "Conformational Analysis. 130. MM2. A Hydrocarbon Force Field Utilizing V1 and V2 Torsional Terms," *Journal of the American Chemical Society*, Vol. 99, No. 25, 1977, pp. 8127-8134. doi:10.1021/ja00467a001

[27] J. Lii and N. L. Allinger, "Molecular Mechanics. The MM3 Force Field for Hydrocarbons. 3. The van der Waals' Potentials and Crystal Data for Aliphatic and Aromatic Hydrocarbons," *Journal of the American Chemical Society*, Vol. 111, No. 23, 1989, pp. 8576-8582. doi:10.1021/ja00205a003

[28] F. Jensen, "Introduction to Computational Chemistry," John Wiley & Sons, Chichester, 1999.

[29] E. V. Kalashnikova, A. V. Kiselev, A. M. Makogon and K. D. Shcherbakova, "Adsorption of Molecules of Different Structure on Graphitized Thermal Carbon Black IV. Gas Chromatographic Investigation of Adsorption of Aldehydes, Ketones and Alcohols on Hydrogen-Treated Graphitized Thermal Carbon Black," *Chromatographia*, Vol. 8, No. 8, 1975, pp. 399-403. doi:10.1007/BF02269088

[30] C. Vidal-Madjar, M. F. Gonnord and G. Guiochon, "Molecular Statistical Theory of Adsorption Prediction of the Thermodynamical Functions of Adsorption of Hydrocarbons on Graphitized Thermal Carbon Black," *Journal of Colloid and Interface Science*, Vol. 52, No. 1, 1975, pp. 102-119. doi:10.1016/0021-9797(75)90306-9

[31] O. G. Eisen, A. V. Kiselev, A. E. Pilt, S. A. Rang and K. D. Shcherbakova, "Gas Chromatographic Investigation of Adsorption of Normal Alkenes C_6 - C_{10} on Graphitized Thermal Carbon Black," *Chromatographia*, Vol. 4, No. 10, 1971, pp. 448-454. doi:10.1007/BF02268813

[32] A. V. Kiselev, E. B. Polotnyuk and K. D. Shcherbakova, "Gas Chromatographic Study of Adsorption of Nitrogen-Containing Organic Compounds on Graphitized Thermal Carbon Black," *Chromatographia*, Vol. 14, No. 8, 1981, pp. 478-483. doi:10.1007/BF02263538

[33] S. N. Yashkin, O. B. Grior'eva and A. K. Buryak, "Experimental and Molecular-Statistical Investigation of Adsorption of Aminoadamantanes on Graphitized Thermal Carbon Black," *Russian Chemical Bulletin*, Vol. 50, No. 6, 2001, pp. 980-985. doi:10.1023/A:1011348730899

[34] S. N. Yashkin, D. A. Svetlov and A. K. Buryak, "Thermodynamic Characteristics of Adsorption of Nitrogen-Containing Heterocycles on Graphitized Thermal Carbon Black Derived from Molecular Statistical Calculation. 1. Azines," *Russian Chemical Bulletin*, Vol. 52, No. 2, 2003, pp. 344-353. doi:10.1023/A:1023446513475

[35] E. G. Bychkova, E. V. Kalashnikova, A. V. Kiselev and K. D. Shcherbakova, "Thermodynamic Characteristics of Adsorption of the Naphthalene-Type Hydrocarbons on the Graphitized Thermal Carbon Black," *Vestnik Moskovskogo Universiteta, Seriya* 2: *Khimiya*, Vol. 27, No. 4, 1986, pp. 382-385.

[36] E. V. Kalashnikova, A. V. Kiselev, R. S. Petrova, K. D. Shcherbakova and D. P. Poshkus, "Chromatographic Measurements and Molecular Statistical Calculations of Thermodynamic Characteristics of Adsorption of Aromatic and Polycyclic Hydrocarbons on Graphitized Thermal Carbon Black," *Chromatographia*, Vol. 12, No. 12, 1979, pp. 799-802. doi:10.1007/BF02260661

[37] E. V. Kalashnikova, A. V. Kiselev and K. D. Shcherbakova, "Retention of Some Phenyl-Substituted and Bicyclic Hydrocarbons on Graphitized Carbon Black," *Chromatographia*, Vol. 17, No. 10, 1983, pp. 521-525. doi:10.1007/BF02261913

[38] A. V. Kiselev, V. I. Nazarova and K. D. Shcherbakova, "Molecular Structure and Retention Behaviour of Some Polycyclic Aromatic and Perhydroaromatic Hydrocarbons on Graphitized Carbon Black," *Chromatographia*, Vol. 18, No. 4, 1984, pp. 183-189. doi:10.1007/BF02276730

[39] E. V. Kalashnikova, A. V. Kiselev, K. D. Shcherbakova and S. D. Vasileva, "Retention of Diphenyls, Terphenyls, Phenylalkanes and Fluorene on Graphitized Thermal Carbon Black," *Chromatographia*, Vol.14, No. 9, 1981, pp. 510-514. doi:10.1007/BF02265630

[40] A. K. Buryak, P. B. Dallakyan and A. V. Kiselev, "Determination of Atom-Atom Potentials of Intermolecular Interaction and Calculation of the Thermodynamic Characteristics of Adsorption on Graphite of Sulfur- and Chlorine-Containing Organic Compounds," *Doklady Akademii Nauk SSSR Physical Chemistry*, Vol. 282, No. 2,1985, pp. 350-353.

[41] A. K. Buryak, A. N. Fedotov and A. V. Kiselev, "Correlation between the Structure of Chlorinated Biphenyls and

Their Adsorption on Graphitized Thermal Carbon Black," *Vestnik Moskovskogo Universiteta*, *Seriya* 2: *Khimiya*, Vol. 26, No. 6, 1985, pp. 568-571.

[42] W. Engewald, E. V. Kalashnikova, A. V. Kiselev, R. S. Petrova, K. D. Shcherbakova and A. L. Shilov, "Gas Chromatographic Investigation of the Adsorption of Polymethylcyclohexanes on Graphitized Thermal Carbon Black," *Journal of Chromatography A*, Vol. 152, No. 2, 1978, pp. 453-466. doi:10.1016/S0021-9673(00)85082-7

[43] T. R. Rybolt and C. E. Wells, "Molecule-Surface Binding Energies from Molecular Mechanics: Nucleobases on Graphene," In: H. E. Chan, Ed., *Graphene and Graphite Materials*, Nova Science Publishers, New York, 2009, pp. 95-112.

[44] C. Thierfelder, M. Witte, S. Blankenburg, E. Rauls and W. G. Schmidt, "Methane Adsorption on Graphene from First Principles Including Dispersion Interaction," *Surface Science*, Vol. 605, No. 7-8, 2011, pp. 746-749. doi:10.1016/j.susc.2011.01.012

[45] O. Engkvist, P. Astrand and G. Karlstrom, "Accurate Intermolecular Potentials Obtained from Molecular Wave Functions: Bridging the Gap between Quantum Chemistry and Molecular Simulations," *Chemical Reviews*, Vol. 100, No. 11, 2000, pp. 4087-4108. doi:10.1021/cr9900477

[46] Y. Zhao and D. G. Truhlar, "Density Functionals for Noncovalent Interaction Energies of Biological Importance," *Journal of Chemical Theory and Computation*, Vol. 3, No. 1, 2007, pp. 289-300. doi:10.1021/ct6002719

[47] R. Zacharia, H. Ulbricht and T. Hertel, "Interlayer Cohesive Energy of Graphite from Thermal Desorption of Polyaromatic Hydrocarbons," *Physical Review B*, Vol. 69, No. 15, 2004, Article ID: 155406. doi:10.1103/PhysRevB.69.155406

[48] H. Ruuska and T. A. Pakkanen, "*Ab Initio* Study of Interlayer Interaction of Graphite: Benzene-Coronene and Coronene Dimer Two-layer Models," *Journal of Physical Chemistry B*, Vol. 105, No. 39, 2001, pp. 9541-9547. doi:10.1021/jp011512i

[49] T. P. Tauer and C. D. Sherrill, "Beyond the Benzene Dimer: An Investigation of the Additivity of π-π Interactions," *Journal of Physical Chemistry A*, Vol. 109, No. 46, 2005, pp. 10475-10478. doi:10.1021/jp0553479

